Circulating Human Interleukin-8 as an Indicator of Cancer Progression in a Nude Rat Orthotopic Human Non–Small Cell Lung Carcinoma Model

Hillary J. Millar,[1] Jeffrey A. Nemeth,[1] Francis L. McCabe,[1] Bill Pikounis,[2] and Eric Wickstrom[3]

[1]Discovery Research, Centocor R&D, Inc., Radnor, Pennsylvania; [2]Nonclinical Statistics, Centocor R&D, Inc., Malvern, Pennsylvania; and [3]Department of Biochemistry and Molecular Biology, Kimmel Cancer Center, Thomas Jefferson University, Philadelphia, Pennsylvania

Abstract

Clinically relevant animal models of human cancer are necessary for the evaluation of putative therapeutics. We hypothesized that circulating human lung cancer–associated proteins would correlate with physiologic measurements from an orthotopic H460 human non–small cell lung carcinoma model that we developed in immunodeficient rats. Physiologic measurements and serum samples were collected over time. Serum interleukin-8 (IL-8), p53, vascular endothelial growth factor, and matrix metalloproteinase-9 were quantitated for correlation with physiologic measurements. Matrix metalloproteinase-9 and p53 were not significantly detectable. Circulating vascular endothelial growth factor was detected at high levels in some tumor-bearing animals. Human IL-8 was detectable in all tumor-bearing animals and correlated positively with markers of respiratory acidosis (pH, $P = 0.012$; TCO_2, $P = 0.024$; pCO_2, $P = 0.007$; and HCO_3^-, $P = 0.029$) and with surface body temperature ($P = 0.001$) beginning on day 16 after implantation. IL-8 levels negatively correlated with survival ($P < 0.001$), indicating an association with tumor burden. Circulating human IL-8 might be a useful, clinically relevant circulating tumor protein marker due to its positive correlation with multiple physiologic variables associated with lung cancer progression. (Cancer Epidemiol Biomarkers Prev 2008;17(8):2180–7)

Introduction

Lung cancer is the leading cause of cancer death in the United States. Currently, there are animal models of human lung cancer that mimic the human disease state (1, 2). However, there are no animal models of human lung cancer that both mimic human disease and show clinically relevant protein biomarker activity. In addition, the majority of orthotopic human lung cancer animal models only use survival as an end point. There is a need for a noninvasive, clinically relevant, efficient, and feasible means to evaluate disease progression in orthotopic human lung cancer animal models. By identifying a protein biomarker that correlates with disease progression, experimental therapeutics may be evaluated for efficacy using the protein activity as an end point rather than survival alone.

Lung cancer is divided into two categories: small cell lung cancer and non–small cell lung cancer (NSCLC), which comprises 85% of all lung cancer. Symptoms of lung cancer include anorexia, acute or chronic respiratory acidosis, wheezing, shortness of breath, and pleural effusion (3-5). Depending on the stage, NSCLC patients may be candidates for surgical resection of the tumor, localized radiation, and chemotherapy. Several factors influence the prognosis of any patient with lung cancer, including the expression of proteins associated with the cancer (6). Large cell lung carcinoma comprises 10% to 15% of all lung cancer (7). The H460 large cell lung carcinoma line is responsive to clinically relevant chemotherapeutics *in vivo* (8). Furthermore, the location (bronchus) of the primary tumor in orthotopic animal models using H460 cells is clinically relevant (9).

Vascular endothelial growth factor (VEGF), matrix metalloproteinase-9 (MMP-9; also known as gelatinase-B), p53, and interleukin-8 (IL-8) are expressed at various levels by NSCLC (10-12). Some studies showed VEGF to be a prognostic marker; plasma and intratumoral VEGF have been shown to correlate with tumor angiogenesis in NSCLC patients (11-14). MMP-9 production is up-regulated and overexpressed in several carcinomas and can be an indication of the success of MMP inhibitor therapy, and plasma and serum MMP-9 levels correlate with NSCLC tumor stage (15-20). p53 mutations are often seen in cancer cells, resulting in loss of cell cycle control and subsequent uncontrolled replication of cancer cells. Cancers expressing p53 mutations often have a poor prognosis; however, the expression of mutant p53 by tumors is not necessarily correlated with tumor size or stage and cannot be used as a serum tumor marker in patients that have late-stage NSCLC (12, 21, 22). Circulating anti-p53 antibodies have been measured in NSCLC patients and are not correlated to disease progression in patients with a positive outcome (23, 24). IL-8, a member of the CXC chemokine family, is

Received 12/19/07; revised 4/29/08; accepted 6/9/08.

Note: Supplementary data for this article are available at Cancer Epidemiology Biomarkers and Prevention Online (http://cebp.aacrjournals.org/).

Requests for reprints: Hillary J. Millar, Discovery Research, Centocor R&D, Inc., Radnor, PA 19087. Phone: 610-240-8727; Fax: 610-651-6152. E-mail: hmillar@cntus.jnj.com

doi:10.1158/1055-9965.EPI-07-2915

produced by NSCLC cells as an autocrine growth factor (25-27).

We hypothesized that circulating levels of lung cancer–associated proteins would correlate with results of physiologic measurements from an orthotopic human NSCLC model in immunodeficient rats. Orthotopic xenograft models restore tumor-host interactions, are more likely to induce distant metastasis, and respond to treatment more like humans, critical to testing novel therapeutics (28). Many standard orthotopic lung cancer models are invasive, such as surgical tracheal exposure or thoracotomy, and inaccurate, such as lateral tail vein or percutaneous intrathoracic injection of cells (28-33).

Here, we report that a noninvasive orthotopic human NSCLC model using H460 cells was developed using the immunodeficient rat. Disease progression and survival were monitored. A clinically relevant chemotherapeutic, docetaxel, was used to validate the model. Several physiologic variables that could be associated with lung function and general health of the animal were explored. To compare the physiologic measurements to the activity of the tumor *in situ*, serum samples were analyzed for tumor expression of human IL-8, MMP-9, p53, and VEGF. Statistically significant correlations between human serum IL-8 and surface body temperature, clinical observations, TCO_2, pH, pCO_2, pO_2, HCO_3^-, BEecf, and sO_2 were found, consistent with the hypothesis.

Materials and Methods

Cell Culture. H460 human large cell lung carcinoma cells (American Type Culture Collection) were derived from the pleural fluid of a patient with large cell cancer of the lung. The H460 cells were maintained in RPMI 1640 containing Glutamax and HEPES-KOH buffer plus 10% fetal bovine serum, 1% nonessential amino acids, and 1% sodium pyruvate. The cells were incubated at 37°C in water-saturated air containing 5% CO_2 and split every 3 d. Cell culture supernatants were harvested 24 h and 5 d after cell seeding. Cell number and viability was determined using a hemocytometer and trypan blue exclusion. Supernatants were frozen at −80°C for subsequent analysis. Two days after medium replenishment, cells were harvested by trypsin/EDTA release for orthotopic implantation. The cell suspension was centrifuged and the pellet was resuspended in Dulbecco's PBS without magnesium or calcium to yield 10^8 cells/mL for an implant of 10^7 cells/0.1 mL per animal.

Animals. Three *in vivo* studies were done to determine the tumor take-rate, responsiveness of the model to standard chemotherapeutic treatment (model validity), and blood analyte and cytokine changes. Female nude rats (Hsd:RH-*Foxn1*^{rnu}), ~5 wk of age, were procured from Harlan Laboratories. The animals were maintained in pairs in microisolator caging and allowed free access to food and water. Environmental conditions consisted of a 12-h light/12-h dark cycle, a temperature of 20°C to 22°C, and a relative humidity of 40% to 60%. Each animal received one-half tablet of 60 mg sulfamethoxazole/10 mg trimethoprim (SCID's MDs, sterile bacon flavored tablets; Bio-Serv) as prophylactic antibiotic treatment beginning 4 d before tumor cell implantation and continuing daily for 2 wk. One day before tumor cell implantation, all animals received 2 cGy whole-body γ-irradiation (Gamma Cell 3000 Elan, MDS Nordion) per gram of body weight. Body weights and clinical observations were recorded twice weekly. Surface body temperature was measured with an IR thermometer (Cole-Parmer) on the abdominal areas of the animals twice weekly. An animal was considered moribund when it developed one or more of the following conditions: body weight loss >15% of the original recorded body weight; surface body temperature below 32°C; and severe ataxia combined with emaciation, limited motor activity, severe gasping, or a crackling sound emanating from the respiratory tract known as rales. On death, the lungs were excised and rinsed in PBS and were perfused with 10% neutral buffered formalin. The animals were maintained in a facility approved by the American Association for Accreditation of Laboratory Animal Care in accordance with current regulations and standards of the U.S. Department of Agriculture. The protocol was reviewed and approved by the Centocor Institutional Animal Care and Use Committee.

Orthotopic Implantation of H460 Cells in Nude Rats. Animals were anesthetized via i.p. injection with 90 mg/kg ketamine/10 mg/kg xylazine and placed in dorsal recumbency on an intubation board (Braintree Scientific, Inc.) at a 45° angle; the head was secured via the upper incisors. A gooseneck lamp was placed perpendicular to the neck to illuminate the trachea. The tongue was gently moved aside and a sterile swab was used to dry the throat. A 0.1 mL cell suspension (10^7 cells) followed by 0.1 mL air was administered into the trachea at the bronchial split using a 1.5-inch, 18-gauge i.v. catheter (BD Angiocath) without stylet. The animals were gently massaged to encourage breathing; body temperature was maintained until they regained consciousness.

Tumor Take-Rate and Survival. Twelve female nude rats were used to determine the establishment rate and time to morbidity of orthotopically implanted H460 cells. Ten animals received intratracheal H460 cells, whereas two animals received intratracheal PBS. Body weights and clinical observations were recorded twice weekly for ~7 wk or when the animals appeared moribund.

Model Validation. Sixteen animals were implanted orthotopically with H460 cells and divided into two groups of eight animals each. Six naive animals were used for comparison. Eight days after cell implantation, the test animals received either 10 mL/kg i.v. saline or docetaxel at a dose of 10 mg/kg on a Q7dx3 schedule. Body weights were recorded twice weekly. The animals were euthanized when moribund or on day 60 after tumor cell implantation.

Blood Analyte and Cytokine Study. Twice weekly for 9 wk (or until animal death), 600 μL of blood were collected from the lateral tail vein of 10 orthotopic H460 tumor-bearing and 9 naive animals. Blood (150 μL) was placed into a lithium heparin tube (Microtainer, Becton Dickinson) for analysis using the i-STAT portable clinical analyzer and CG4+ cartridges (Heska). Blood lactate, total carbon dioxide (TCO_2), pH, partial pressure of carbon dioxide (pCO_2), partial pressure of oxygen (pO_2), bicarbonate (HCO_3^-), base excess (BEecf), and oxygen saturation (sO_2) were measured. Blood (450 μL) was placed into a serum separator tube (Capiject, Terumo) for

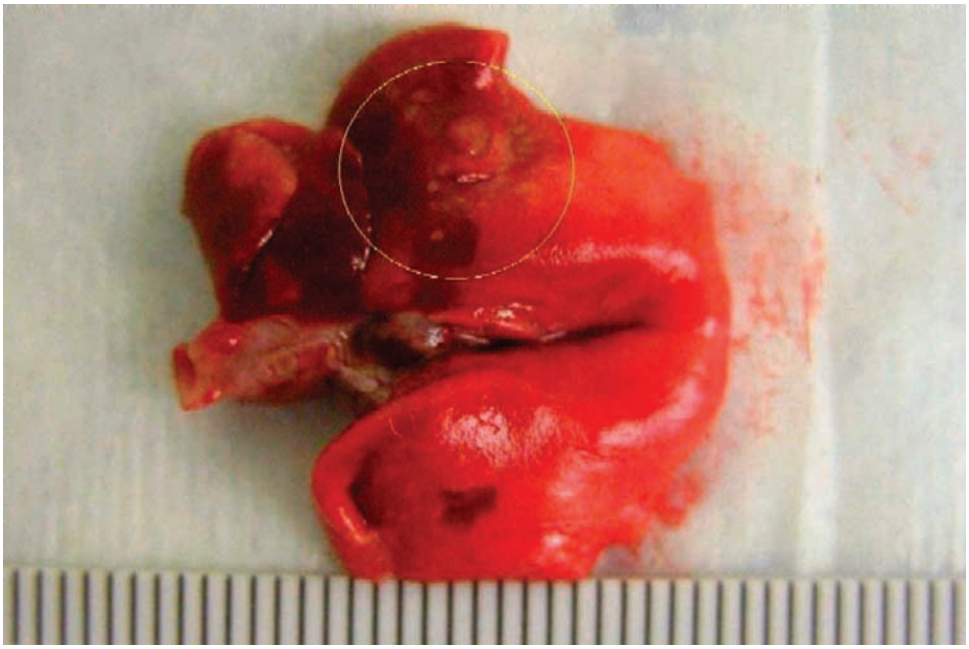

Figure 1. Gross tumor nodules (*circled*) in the lungs of the surviving tumor-bearing animal on day 48 after tumor cell implantation. Rats were anesthetized and received either intratracheal PBS or 1×10^7 H460 cells. Scale is millimeters.

serum protein analysis. Serum was separated and frozen at −80°C until analyzed. One to two fresh blood droplets were used for prandial glucose measurements using a One Touch Ultra glucometer (LifeScan) with code 9 test strips. The study was terminated on day 62 after implantation.

Serum and Supernatant Protein Analysis. Human cytokine Multiplex Bead Immunoassay kits were obtained from BioSource Invitrogen, Inc. BioSource designed a custom multiplex kit for specific detection of human total p53, IL-8, and VEGF. A MMP 3-plex was used for detection of human MMP-9. The cytokine standards provided with the kits had expected detectable concentrations of 0 to 15.11 ng/mL (human VEGF), 0 to 6.59 ng/mL (human IL-8), 0 to 7.69 ng/mL (human p53), and 0 to 42 ng/mL (human MMP-9). The Bio-Rad Bio-Plex 200 system and software were used to read the multiplexes. The Bio-Plex machine was calibrated before each use using Bio-Rad calibration beads.

Serum was thawed to room temperature and centrifuged at 13,200 rpm (19,495 × *g*) for 10 min. Briefly, standards were diluted in assay diluent (provided in the kits), and neat serum samples were plated. Samples were incubated for 2 h with antibody-conjugated beads on an orbital shaker and washed. Samples were then incubated with biotinylated antibody for 1 h on an orbital shaker and washed. Samples were incubated with streptavidin–R-phycoerythrin for 30 min, washed twice, and analyzed.

H460 cell supernatant was thawed at 4°C refrigeration overnight. The supernatant was centrifuged at 3,500 rpm (1,370 × *g*) for 10 min to pellet any debris. Standards and samples were diluted in 50% assay diluent and 50% cell culture medium. Standards and samples were plated, incubated, and analyzed as described previously.

Immunohistochemistry. Naive rat lung samples were used as negative control tissues, and known positive control tissues for each protein of interest were stained using the i6000 Automated Staining System (BioGenex). The lung samples were perfused and fixed with 10% neutral buffered formalin. Tissues were embedded in paraffin blocks before sectioning. Mouse anti-human IL-8 (GeneTex, Inc.), mouse anti-human VEGF (R&D Systems, Inc.), mouse anti-human MMP-9, clone 4H3 antibody (R&D Systems), and mouse anti-human p53 (GeneTex) antibodies were used to detect human IL-8, VEGF, MMP-9, and p53 (respectively) in the rat lungs. Mouse IgG (BioGenex) was used as the negative control antibody, and biotinylated rat-absorbed horse anti-mouse IgG (Vector Laboratories) was used as the secondary antibody.

Paraffin sections (5 μm) were stained using the standard avidin-biotin complex. Briefly, sections were blocked for endogenous peroxidase activity and protein and incubated for 1 h with primary antibody, 30 min with secondary antibody, streptavidin for 20 min, 3,3′-diaminobenzidine for 10 to 20 min, and Mayer's hematoxylin (to counterstain) for 2 min. Slides were rinsed in running tap water for 5 min before dehydration and mounting. Antigen retrieval by microwave and decloaking was used for VEGF and p53 detection.

Statistical Analysis. Kaplan-Meier survival analysis at 95% confidence interval was used to analyze survival in all *in vivo* experiments. Full repeated measures analysis was used for pairwise comparisons between the tumor-bearing animals and naive or control animals when analyzing in-life measurements and blood analyte values. Mixed-effects statistical models (34) were fit to the data, accounting for within-subject variability, correlations, and the between-subject variability. Natural splines (35) were used to flexibly characterize the time profiles through day 23, as deaths in the tumor-bearing group occurred thereafter. The logarithmic scale of end points was used in the model fits to better satisfy underlying statistical model assumptions of equal variance, normal distribution, and uniform correlation. Use of the log scale also facilitates the estimation of

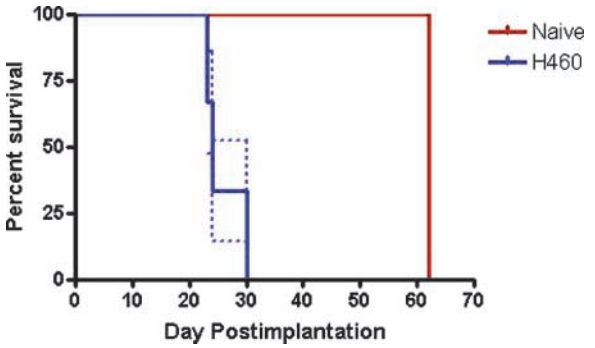

Figure 2. Survival of naive and tumor-bearing animals. Naive animals were euthanized on day 62 after tumor cell implantation. Tumor-bearing animals survived for 26 ± 4 d after tumor cell implantation.

differences in terms of percent. Pairwise comparisons between the naive and tumor-bearing animal groups were made at each time point, and P values of <0.05 were deemed significant. For correlations among the different analyte end points, Spearman's index and test was used after calculating the mean across time points for each subject. Correlations and tests of analytes with survival outcomes were estimated by fitting Cox regression models to evaluate how the hazard probability of death was affected. All calculations and graphs were done in the R software environment (36).

Results

Tumor Take-Rate and Survival. We determined the tumor establishment rate and survival associated with the orthotopic tumors. Ten animals received 1×10^7 intratracheal H460 cells, and two animals received intratracheal PBS. Nine of 10 H460-bearing animals became moribund and were euthanized before study termination (day 48). One tumor-implanted animal survived until day 48 and was found to have lung tumors at necropsy (Fig. 1). Tumor-bearing animals were found to have a significantly shorter survival time (P = 0.0473, Kaplan-Meier survival analysis; data not shown) despite one animal living until the end of the study.

Model Validation. An important characteristic of animal models is an expected response to standard therapeutics. A study was designed to test the efficacy of docetaxel in this model. Sixteen animals received intratracheal H460 cells and 6 animals remained naive. The 16 implanted animals were randomized into two groups of eight: one group received i.v. saline and the other group received i.v. docetaxel at 10 mg/kg once weekly for three doses. Docetaxel-treated animals survived significantly longer (45 ± 15 days) than saline-treated animals (24 ± 15 days; P = 0.0048, Kaplan-Meier survival analysis; data not shown).

Clinical Observations, Blood Analyte, and Cytokine Study. Nine naive animals and 10 tumor-bearing animals were used to correlate various in-life measurements with serum tumor proteins. Lungs were harvested from tumor-bearing animals on the day of death (days 23-30 after tumor cell implantation; Fig. 2). The lungs were removed, weighed, and processed as described previously. Wet lung weights from tumor-bearing animals were not significantly different from those of naive animals (P = 0.485; data not shown). Four of 10 animals implanted with tumor cells did not become moribund and were euthanized on day 62 after tumor cell implantation. At necropsy, there was no gross evidence of tumors in the lungs, and all data associated with these animals were censored for statistical analysis; the remaining six animals had gross tumor nodules ranging from 0.5 to 3 mm in diameter. Naive animals survived significantly longer than tumor-bearing animals (P < 0.0001, Kaplan-Meier survival analysis; Fig. 2).

Clinical observations, body weights, and surface body temperature were measured for all animals twice weekly throughout the study. Starting on day 20 and continuing throughout the study, the H460 implanted animals exhibited wheezing, severe gasping and dyspnea, loss of body weight, hypothermia, and ataxia. Repeated measures analysis of surface body temperature showed that tumor-bearing animals had an increasingly lower surface body temperature in comparison with naive animals, reaching significance on day 16 (Table 1). Additionally, there was a significant reduction in the body weight of the six tumor-bearing animals versus the naive animals on days 20 and 23 (Table 1).

There were significant correlations (P < 0.05) between survival and surface body temperature, body weight, and clinical observations 23 days after tumor cell implantation. As the incidence of clinical observations increased, there was a strong correlation with death

Table 1. Animal surface body temperature and body weight change

Day after implantation	Surface body temperature (°F)					Body weight change (%)				
	N		T		P	N		T		P
	Mean	SE	Mean	SE		Mean	SE	Mean	SE	
2	96	0.3	95.5	0.4	0.262	NA	NA	NA	NA	NA
8	96.7	0.2	96.2	0.3	0.147	1.05	0.02	1.06	0.02	0.68
12	97.4	0.2	96.9	0.3	0.156	1.1	0.01	1.12	0.02	0.428
16	97.7	0.3	96.8	0.3	*0.32*	1.14	0.02	1.15	0.02	0.887
20	97.4	0.2	95.8	0.3	*<0.001*	1.18	0.01	1.013	0.02	*0.034*
23	96.9	0.3	94.6	0.4	*<0.001*	1.19	0.02	1.09	0.02	*<0.001*

NOTE: Means, SEs, and P values of tumor-bearing versus naive animals. In-life measurements were recorded twice weekly throughout the study for correlation with serum protein concentration. Italicized P values are significant.
Abbreviations: N, naive; T, tumor bearing; NA, not available.

Table 2. Day 23 after tumor cell implantation blood analyte and gas correlation with survival

Variable	*P*	Correlation coefficient
Lactate	0.195	0.72
TCO_2	*<0.001*	0.61
pH	*0.001*	−47.89
pCO_2	*<0.001*	0.21
pO_2	*0.013*	−0.27
HCO_3^-	*<0.001*	0.62
BEecf	*0.001*	0.53
sO_2	*0.005*	−0.16
Glucose	*0.003*	0.10

NOTE: Italicized *P* values are significant.

($P < 0.001$). There was a significant correlation between death and a reduction in surface body temperature and body weight ($P < 0.001$ and $P = 0.014$, respectively). Naive animals survived significantly longer than tumor-bearing animals ($P < 0.001$, Kaplan-Meier survival analysis; data not shown for this paragraph).

Blood Analyte Measurements. Prandial blood glucose, lactate, TCO_2, pH, pCO_2, pO_2, HCO_3^-, BEecf, and sO_2 were measured twice weekly (on the day of clinical observations and body weights) from whole blood samples collected using lateral tail vein venipuncture (Table 2). Repeated measures analyses at a 95% confidence interval of tumor-bearing animals versus naive animals ended when tumor-bearing animals began to die (day 23 after tumor cell implantation).

There was no significant difference in lactate values of tumor-bearing versus naive animals. TCO_2 values were increasingly significant in tumor-bearing versus naive animals starting on day 16 ($P = 0.006$) and continuing to day 23 ($P < 0.001$). There was a significant difference in pH values of tumor-bearing versus naive animals on days 8 ($P = 0.029$), 12 ($P = 0.015$), 20 ($P = 0.019$), and 23 ($P = 0.013$). pCO_2 values were increasingly significant in tumor-bearing versus naive animals beginning on day 8 ($P = 0.032$) and continuing to day 23 ($P < 0.001$), with the exception of day 16. pO_2 values were significantly lower in tumor-bearing versus naive animals on days 20 and 23 ($P = 0.012$, each day) after tumor cell implantation. There was an increasingly significant difference in HCO_3^- values of tumor-bearing versus naive animals beginning on day 16 ($P = 0.010$), continuing to day 23 ($P < 0.001$). BEecf values were significantly higher in tumor-bearing versus naive animals on days 20 ($P = 0.008$) and 23 ($P = 0.018$). sO_2 values were significantly lower in tumor-bearing versus naive animals on days 20 and 23 ($P < 0.001$, each day), with values approaching significance on day 16. There were no significant differences in glucose values of tumor-bearing versus naive animals; however, values approached the 0.05 significance level on days 20 and 23 (Supplementary Table S3).

When the blood analyte values were averaged across time points for each animal, significant correlations were seen. Base excess, the amount of base that must be added to restore pH to normal levels, was elevated in the tumor-bearing group compared with the naive group and found to be significantly positively correlated to TCO_2 ($P < 0.001$), pCO_2 ($P < 0.001$), and HCO_3^- ($P < 0.001$) and inversely correlated to pH ($P = 0.021$), pO_2 ($P = 0.001$), and sO_2 ($P = 0.001$).

Several blood gas and analyte values significantly correlated with survival at 95% confidence. On day 23 after tumor cell implantation, increasing TCO_2, pCO_2, HCO_3^-, BEecf, and glucose values, and decreasing pH, pO_2, and sO_2, correlated with death. Lactate was not significantly correlated to survival (Table 2).

Cytokine Analysis. The presence of human MMP-9, p53, IL-8, and VEGF in the culture supernatant of H460 cells was examined using multiplex bead immunoassays. Twenty-four hours after seeding, human VEGF, IL-8, and p53 were detected at low levels in all the flasks. Five days later, IL-8 increased by 2-fold, whereas VEGF and p53 were 6-fold higher. MMP-9 was not detected in the supernatants (Supplementary Tables S4-S6). There were strong correlations between cell number and supernatant protein concentration (IL-8, $r = 0.9983$; VEGF, $r = 0.9970$; and p53, $r = 0.9983$; Supplementary Figs. S4 and S5).

Next, the relationship between human MMP-9, p53, IL-8, and VEGF in the mouse serum and changes in clinical signs and blood analytes was determined. The average values of analytes across the time points for each animal were correlated to the average values of serum proteins across the time points for each animal at 95% confidence. There was no significant correlation between serum p53 and any blood analyte, gas, or in-life measurement. MMP-9 was not detected in the serum.

In tumor-bearing animals, there was a gradual increase in serum IL-8 beginning on day 16 after tumor

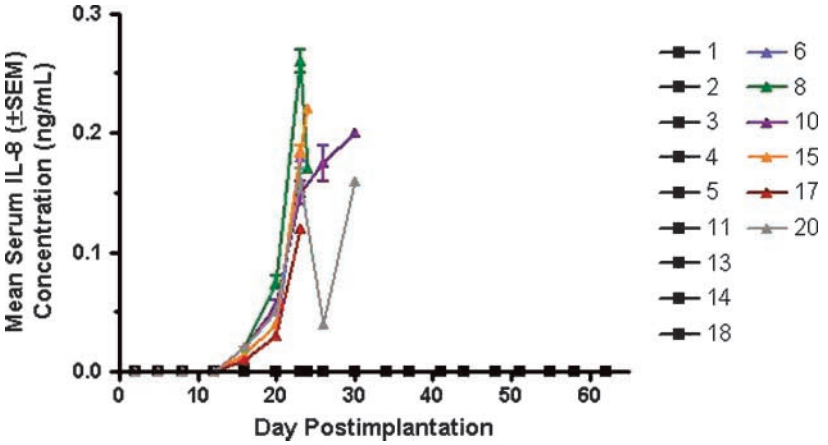

Figure 3. Days after tumor cell implant versus serum IL-8 levels (ng/mL) ± SE in individual naive (■) and tumor-bearing (▲) animals. Serum was collected from all animals twice weekly and analyzed in duplicate using a multiplex bead immunoassay. There is a gradual increase in serum IL-8 concentration among tumor-bearing animals beginning on day 16 and continuing until death.

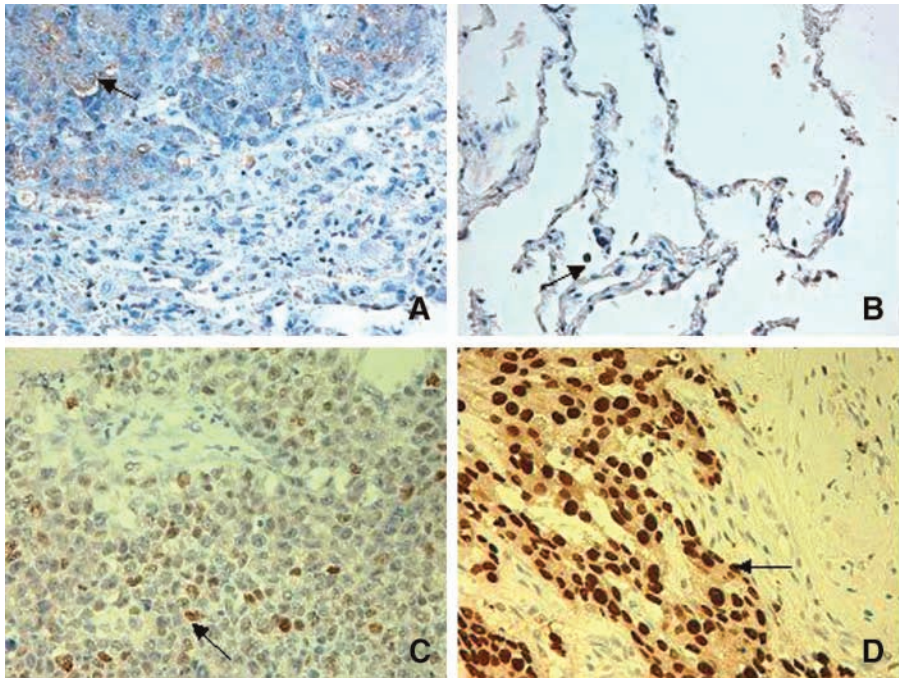

Figure 4. H460 tumor in immunocompromised rat lung. **A.** Positive membrane and cytoplasmic staining of human IL-8 can be seen in the tumor cells on the upper half of the photograph. **B.** Normal human lung positive control with positive cytoplasmic staining of human IL-8 in alveolar macrophages. Magnification, ×40. **C.** Positive nuclear staining of human p53 can be seen in the tumor cells. Magnification, ×40. Human breast adenocarcinoma was used as a positive control for p53. **D.** Human breast adenocarcinoma positive control with positive nuclear and cytoplasmic staining of human p53 in tumor cells. Magnification, ×40.

cell implantation, continuing until death (Fig. 3). IL-8 correlated positively and significantly with TCO_2 ($P = 0.024$), PCO_2 ($P = 0.007$), HCO_3^- ($P = 0.029$), and the occurrence of clinical symptoms (gasping, rales, etc.; $P < 0.001$). IL-8 correlated inversely but significantly with blood pH ($P = 0.012$) and surface body temperature ($P = 0.001$). Both IL-8 and surface body temperature grew increasingly significant until day 23 (Supplementary Table S7).

VEGF correlated positively and significantly with the occurrence of clinical symptoms ($P = 0.028$). On day 23 after tumor cell implantation, both VEGF and IL-8 correlated positively and significantly with survival ($P < 0.001$; Supplementary Table S7). p53 and MMP-9, however, did not correlate significantly with survival ($P = 0.317$ and 1.000, respectively; data not shown).

Immunohistochemical Detection of Human IL-8, p53, VEGF, and MMP-9. Lung sections from all animals were immunostained for human IL-8, VEGF, MMP-9, and p53. For human IL-8 staining, a dark brown precipitate in the tumor cell cytoplasm and membranes indicated positive staining. Areas of heavy staining were seen within the tumors, and no staining was seen in nearby bronchus-associated lymphoid tissue or normal tissue. Most of the staining was confined to the tumor cell and vacuole membranes, with minimal cytoplasmic staining and no background staining (Fig. 4A). The primary and secondary antibody control slides and naive rat lung tissue slides were negative for staining. The positive control tissue, normal human lung, had positive staining in alveolar macrophages (Fig. 4B). For human p53 staining, positive staining appeared as a dark brown precipitate in the nucleus of tumor cells for the H460-bearing nude rat lung and the positive control (Fig. 4C and D, respectively) human breast adenocarcinoma. The naive nude rat lung tissue and primary and secondary antibody control tissues were negative for staining. For human VEGF detection, an optimal staining protocol could not be defined. For human MMP-9 staining, a dark brown precipitate in the tumor cell cytoplasm indicated positive staining. There was positive staining of necrotic tumor cells only in the H460-bearing lung tissue (most likely background staining) and positive control tissue and no staining of the naive animal tissue (Supplementary Figs. S6-S8). It was concluded that MMP-9 was not present at detectable levels in the tumor for staining.

Discussion

We have developed and validated an immunocompromised rat orthotopic model of human large cell lung carcinoma and correlated the presence of circulating exogenous xenograft tumor marker proteins with disease progression. It was found that the orthotopic implantation of human large cell lung carcinoma cells into the tracheal airway of the nude rat produced a viable and feasible model of NSCLC lung cancer. Although there were definite clinical signs that were associated with survival, each animal displayed an independent disease process, similar to that seen in man. Animals that were able to initially adapt to the disease and succumbed to the disease later than other animals were found to have a greater tumor burden, whereas those that were moribund early in the studies and were euthanized showed less tumor burden. This variability in survival and tolerance to the symptoms and disease process associated with lung cancer mimic the clinical setting.

Tumor xenograft-secreted human IL-8 was identified as the most abundant and predictive circulating tumor marker protein that correlated with cancer progression in the animal model. Circulating IL-8 was limited to the tumor-bearing animals and was detectable beginning on day 16, continuing to rise until the day of death. Although circulating human IL-8 concentration

correlated to several blood analyte values and surface body temperature, the presence of IL-8 and the blood measurements are most likely independent events.

IL-8 immunostaining in the tumor-bearing rat lung seemed to be heterogeneous, which is expected in tumor tissue. It was clearly present within the tumor, associated with cell membranes and vacuole-like structures. Cytoplasmic staining was seen in the alveolar macrophages of the positive control human lung tissue. Alveolar macrophages are known to secrete IL-8 as a neutrophil activator and chemoattractant (25, 26). In addition to being a motogenic factor, IL-8 is also mitogenic and angiogenic (27). IL-8 and its receptors, CXCR1 and CXCR2, are coexpressed in H460. H460 cell growth can be stimulated by exogenous IL-8, leading to the belief that it is an autocrine growth factor. CXCR1 and CXCR2 are both cell surface receptors (37). The staining of tumor-bearing rat alveolar macrophages was most likely due to phagocytosis of IL-8–positive H460 cells. Cell culture supernatant showed high expression of IL-8, p53, and VEGF by the H460 cells. The increasing levels of IL-8 may be correlated with the rate of replication of the tumor cells because the number of cells on day 5 after seeding was nearly double that at 24 h after seeding, and the concentration of IL-8 approximately doubled as well. The production of IL-8 by the cells in culture was most likely to continue mitogenic and angiogenic activity, as mentioned in Introduction.

At day 5 after seeding, there was a high percentage of cell death, which may explain the high levels of p53 in the supernatant. Although circulating p53 values of tumor-bearing animals were not statistically different from naive animals, suggesting its absence in circulation, positive staining of the p53 protein was seen in the H460 tumors growing in the rat lungs. Because p53 is a nuclear protein, it can be assumed that circulating p53 would be detected if the tumor cells were apoptotic or dying (as in chemotherapy treatment). It would be interesting to quantitate circulating human p53 in this animal model during treatment with a cytotoxic therapeutic. MMP-9 was not detected in the serum samples or the H460 lung tumors. The positive control (human lung) staining was confluent in lung epithelial cells and alveolar macrophages, consistent with reports of overexpression of MMP-9 by alveolar macrophages in lung disease such as chronic obstructive pulmonary disease, increasing the elastolytic load of the lung in response to the inflammatory stimulus (38). Because MMP-9 is primarily a stromal matrix protein, it was somewhat expected to see negative results for serum analysis and immunohistochemistry. A more favorable approach would have been to quantitate rat MMP-9 and compare levels between tumor-bearing and naive animals.

VEGF could not be detected in H460 tumors by immunohistochemistry; however, elevated levels were seen in the serum of some H460-bearing animals on the day of death. This may correlate with previous findings of VEGF and IL-8 interaction in tumor progression. Chelouche-Lev et al. (39) showed that breast cancer cell lines that overexpress VEGF also express high levels of IL-8. Additionally, VEGF and IL-8 gene promoter regions both contain recognition sites for activator protein-1 and are coactivated during key angiogenic periods in head and neck squamous cell carcinoma growth (40). The detection of serum VEGF in this animal model could be optimized using a more sensitive assay such as ELISA, in which background values could easily be subtracted out.

Surface body temperature did not show a significant correlation with IL-8 until day 20, indicating that it is independent of IL-8. Furthermore, it has been shown that human IL-8 does not cross-react and is not homologous with rat IL-8 and its receptors. However, the same investigation showed that rat neutrophil recruitment as a result of intratracheal introduced human IL-17 could increase rat IL-8 (41). If H460 cells produced human IL-17, rat IL-8 may increase and there could be a downstream inflammatory response. However, this is not likely the case, as it has been shown that IL-17 is specifically derived from T lymphocytes and activated monocytes (42, 43). TCO_2, PCO_2, and HCO_3^- were already known to be positively correlated with each other and inversely correlated to pH, as part of a respiratory acidosis. Respiratory acidosis occurs when there is hypoventilation in the pulmonary alveoli, thus raising the arterial CO_2 concentration. The buildup of carbonic acid formed from blood CO_2 and water lowers blood pH. To regulate blood pH, cellular bicarbonate is released, and a near-normal pH is achieved. A similar trend was seen in the tumor-bearing animals. On day 23 after tumor cell implantation (the last day of statistical analysis), TCO_2 of tumor-bearing animals was as high as 48 mmol/L compared with the highest naive animal value, 33 mmol/L. On the same day, tumor-bearing animal blood pH was as low as 7.307, and the lowest naive animal pH at 7.384. Normal rat arterial pH is 7.38 ± 0.02 (44). An inverse correlation was found between TCO_2 and pH. Bicarbonate was elevated in the tumor-bearing animals, as high as 44.9 mmol/L, and in the naive group as high as 31.8 mmol/L. Again, an inverse correlation was found between pH and bicarbonate.

An orthotopic human lung cancer model, using H460 human large cell lung carcinoma, has been successfully developed and validated, and a tumor protein marker, IL-8, that correlates with clinical symptoms and blood gas measurements has been identified. Further development and characterization of the model will include immunohistochemical detection of rat MMP-9 expression by tumor stromal cells, and the evaluation of more accurate methods of quantifying tumor burden in the lungs such as PCR. The model will be used in the development of putative cancer therapeutics. It has not been shown that serum IL-8 will correlate with tumor burden in the presence of therapeutic treatment. The effect of treatment on tumor-associated serum IL-8 will be evaluated with each therapeutic due to the differing mechanisms of action associated with the therapies.

Disclosure of Potential Conflicts of Interest

No potential conflicts of interest were disclosed.

Acknowledgments

The costs of publication of this article were defrayed in part by the payment of page charges. This article must therefore be hereby marked *advertisement* in accordance with 18 U.S.C. Section 1734 solely to indicate this fact.

References

1. Wu W, Onn A, Isobe T, et al. Targeted therapy of orthotopic human lung cancer by combined vascular endothelial growth factor and epidermal growth factor receptor signaling blockade. Mol Cancer Ther 2007;6:471–83.
2. Shi J, Zheng D, Liu Y, et al. Overexpression of soluble TRAIL induces apoptosis in human lung adenocarcinoma and inhibits growth of tumor xenografts in nude mice. Cancer Res 2005;65:1687–92.
3. Wikipedia Foundation, Inc. Respiratory acidosis. St. Petersburg (FL): Wikipedia Foundation, Inc.; 2006.
4. Kaufman DA. Respiratory acidosis. New York: Medical Encyclopedia; 2006.
5. Merck & Co., Inc. Lung cancer. Whitehouse Station (NJ): Merck & Co., Inc.; 2003.
6. National Cancer Institute. Non-small cell lung cancer: treatment. Bethesda (MD): National Cancer Institute; 2006.
7. American Cancer Society, Inc. What is non-small cell lung cancer? Atlanta (GA): American Cancer Society, Inc.; 2006.
8. Kraus-Berthier L, Jan M, Guilbaud N, Naze M, Pierré A, Atassi G. Histology and sensitivity to anticancer drugs of two human non-small cell lung carcinomas implanted in the pleural cavity of nude mice. Clin Cancer Res 2000;6:297–304.
9. Wigle D, Liu J, Johnston M. *In vivo* systems for studying cancer. Cancer Treat Res 2007;137:24–43.
10. Boldrini L, Gisfredi S, Ursino S, et al. Interleukin-8 in non-small cell lung carcinoma: relation with angiogenic pattern and p53 alterations. Lung Cancer 2005;50:309–17.
11. Ferrara N, Davis-Smyth T. The biology of vascular endothelial growth factor. Endocr Rev 1997;18:4–25.
12. Zhu C-Q, Shih W, Ling C-H, Tsao M-S. Immunohistochemical markers of prognosis in non-small cell lung cancer: a review and proposal for a multiphase approach to marker evaluation. J Clin Pathol 2006;59:790–800.
13. Masuya D, Huang C-I, Liu D, et al. The intratumoral expression of vascular endothelial growth factor and interleukin-8 associated with angiogenesis in non-small cell lung carcinoma patients. Cancer 2001; 92:2628–38.
14. Tamura M, Ohta Y, Kajita T, et al. Plasma VEGF concentration can predict the tumor angiogenic capacity in non-small cell lung cancer. Oncol Rep 2001;8:1097–102.
15. Illemann M, Bird N, Majeed A, et al. MMP-9 is differentially expressed in primary human colorectal adenocarcinomas and their metastases. Mol Cancer Res 2006;4:293–302.
16. Jinga DC, Blidaru A, Condrea I, et al. MMP-9 and MMP-2 gelatinases and TIMP-1 and TIMP-2 inhibitors in breast cancer: correlations with prognostic factors. J Cell Mol Med 2006;10:499–510.
17. Koç M, Ediger D, Budak F, et al. Matrix metalloproteinase-9 (MMP-9) elevated in serum but not in bronchial lavage fluid in patients with lung cancer. Tumori 2006;92:149–54.
18. Sienel W, Hellers J, Morresi-Hauf A, et al. Prognostic impact of matrix metalloproteinase-9 in operable non-small cell lung cancer. Int J Cancer 2003;103:647–51.
19. Ondo K, Sugio K, Yamazaki K, et al. The significance of serum active matrix metalloproteinase-9 in patients with non-small cell lung cancer. Lung Cancer 2004;46:205–13.
20. Bugdayci G, Kaplan T, Sezer S, et al. Matrix metalloproteinase-9 in broncho-alveolar lavage fluid of patients with non-small cell lung cancer. Exp Oncol 2006;28:169–71.
21. Somasundaram K. Tumor suppressor p53: regulation and function. Front Biosci 2000;5:424–37.
22. Sen E, Akar N. The detection of quantitative serum p53 protein in lung cancer. Tuberk Toraks 2005;53:231–7.
23. Liu Y, Kulesz-Martin M. P53 regulation and function in normal cells and tumors. Medicina 2000;60:9–11.
24. Bergqvist M, Brattström D, Larsson A, Hesselius P, Brodin O, Wagenius G. The role of circulating anti-p53 antibodies in patients with advanced non-small cell lung cancer and their correlation to clinical parameters and survival. BMC Cancer 2004;4:66.
25. Pantelidis P, Southcott AM, Black CM, Du Bois RM. Up-regulation of IL-8 secretion by alveolar macrophages from patients with fibrosing alveolitis: a subpopulation analysis. Clin Exp Immunol 1997;108:95–104.
26. Xie K. Interleukin-8 and human cancer biology. Cytokine Growth Factor Rev 2001;12:375–91.
27. Arenberg DA, Kunkel SL, Polverini PJ, et al. Inhibition of interleukin-8 reduces tumorigenesis of human non-small cell lung cancer in SCID mice. Eur J Clin Invest 1996;97:2792–802.
28. Myers JN, Holsinger C, Jasser SA, Bekele BN, Fidler IJ. An orthotopic nude mouse model of oral tongue squamous cell carcinoma. Clin Cancer Res 2002;8:293–8.
29. Onn A, Isobe T, Itasaka S, et al. Development of an orthotopic model to study the biology and therapy of primary human lung cancer in nude mice. Clin Cancer Res 2003;9:5532–9.
30. Cuenca RE, Takita H, Bankert R. Orthotopic engraftment of human lung tumors in SCID mice for the study of metastasis. Surg Oncol 1996;5:85–91.
31. Howard RB, Chu H, Zeligman BE, et al. Irradiated nude rat model for orthotopic human lung cancers. Cancer Res 1991;51:3274–80.
32. McLemore TL, Eggleston JC, Shoemaker RH, et al. Comparison of intrapulmonary, percutaneous intrathoracic, and subcutaneous models for the propagation of human pulmonary and nonpulmonary cancer cell lines in athymic nude mice. Cancer Res 1988;48:2880–6.
33. Zou Y, Fu H, Ghosh S, Farguhar D, Klostergaard J. Antitumor activity of hydrophilic paclitaxel copolymer prodrug using locoregional delivery in human orthotopic non-small cell lung cancer xenograft models. Clin Cancer Res 2004;10:7382–91.
34. Pinheiro JC, Bates DM. Mixed-effects models in S and S-PLUS. New York: Springer-Verlag; 2000.
35. de Boor C. A practical guide to splines. New York: Springer-Verlag; 1978.
36. Sterovetta R. A language and environment for statistical computing. Vienna (Austria): R Foundation for Statistical Computing; 2006.
37. Zhu YM, Webster SJ, Flower D, Woll PJ. Interleukin-8/CXCL8 is a growth factor for human lung cancer cells. Br J Cancer 2004;91: 1970–6.
38. Russell RE, Culpitt SV, DeMatos C, et al. Release and activity of matrix metalloproteinase-9 and tissue inhibitor of metalloproteinase-1 by alveolar macrophages from patients with chronic obstructive pulmonary disease. Am J Respir Cell Mol Biol 2002;26:602–9.
39. Chelouche-Lev D, Millar CP, Tellez C, Ruiz M, Bar-Eli M, Price JE. Different signaling pathways regulate VEGF and IL-8 expression in breast cancer: implications for therapy. Eur J Cancer 2004;40:2509–18.
40. Bancroft C, Chen Z, Dong G, et al. Coexpression of proangiogenic factors IL-8 and VEGF by human head and neck squamous cell carcinoma involves coactivation by MEK-MAPK and IKK-NF-κB signal pathways. Clin Cancer Res 2001;7:435–42.
41. Laan M, Cui Z-H, Hoshino H, et al. Neutrophil recruitment by human IL-17 via C-X-C chemokine release in the airways. J Immunol 1999;162:2347–52.
42. Fujino S, Andoh A, Bamba S, et al. Increased expression of interleukin 17 in inflammatory bowel disease. Gut 2003;52:65–70.
43. Starnes T, Robertson MJ, Sledge G, et al. Cutting edge: IL-17F, a novel cytokine selectively expressed in activated T cells and monocytes, regulates angiogenesis and endothelial cell cytokine production. J Immunol 2001;167:4137–40.
44. Bailey JL, England BK, Long RC, Jr., Weissman J, Mitch WE. Experimental acidemia and muscle cell pH in chronic acidosis and renal failure. Am J Physiol Cell Physiol 1995;269:C706–12.

Circulating Human Interleukin-8 as an Indicator of Cancer Progression in a Nude Rat Orthotopic Human Non–Small Cell Lung Carcinoma Model

Hillary J. Millar, Jeffrey A. Nemeth, Francis L. McCabe, et al.

Cancer Epidemiol Biomarkers Prev 2008;17:2180-2187.